# Dynamics of delaminated smart composite cross-ply beams

Smart Mater. Struct. **8** (1999) 92–99. Printed in the UK PII: S0964-1726(99)99061-4

# Dynamics of delaminated smart composite cross-ply beams

**Aditi Chattopadhyay†, Dan Dragomir-Daescu‡ and Haozhong Gu§**

Department of Mechanical and Aerospace Engineering, Arizona State University, Tempe, AZ, USA

Received 6 April 1998, in final form 2 November 1998

**Abstract.** A refined higher order theory-based finite element model is presented for modeling the dynamic response of delaminated smart composite cross-ply beams. The refined displacement field accurately accounts for transverse shear deformations through the thickness, and all traction-free boundary conditions are satisfied at all free surfaces including delamination interfaces. The developed theory provides an accurate, computationally efficient analysis tool for the study of smart composite cross-ply beams with piezoelectric sensing and actuation in the presence of delamination. The theory is implemented using the finite element method to allow the incorporation of practical geometries, boundary conditions and the presence of discrete piezoelectric transducers.

A new formulation is presented to include nonlinear induced strain effects. Vibration control is accomplished by piezoelectric layers incorporated in the composite beam. The resulting finite element model is shown to agree well with published experimental data, and the results show significant improvements compared to existing analytical solutions. Numerical results presented in the paper indicate changes in natural frequencies, mode shapes and dynamic responses due to delaminations.

## 1. Introduction

Recently, smart composite structures have received considerable attention due to the potential for designing adaptive structures which are both light in weight and possess adaptive control capabilities for shape correction and vibration control. In designing with composites, it is important to take into consideration imperfections, such as delaminations, that are often pre-existing or are generated by external impact forces during the service life. The existence of delamination can significantly alter the dynamic response of composite structures. Several mathematical models have been reported in the literature for the analysis of beams and plates with piezoelectric sensing/actuation. The classical theory-based approach (Crawley and Anderson 1989, Lee 1990) was first introduced to investigate such a problem with thin plates. This was followed by the first order Mindlin type analyses (Chandrashekhara and Agarwal 1993, Tzou and Zhong 1993) and the potentially expensive layer-wise theories (Robbins and Reddy 1991, Lee and Saravanos 1995). A hybrid theory has also been reported (Mitchell and Reddy 1995). It is well known that refined higher order theories are capable of capturing the transverse shear deformation through the thickness quite accurately (Chattopadhyay and Gu 1994). These theories are applicable to laminates of thicker construction and have been shown to be useful in modeling smart composite laminates (Reddy 1990, Chattopadhyay and Seeley 1996, 1997). Finite element based solution procedures (Chandrashekhara and Agarwal 1993, Robbins and Reddy 1991, Chattopadhyay and Seeley 1996) are practical since real geometries and boundary conditions can be investigated.

A significant amount of research has also been performed in modeling delamination in composites. Although three-dimensional approaches (Yang and He 1994, Whitcomb 1989) are more accurate than two-dimensional theories (Pavier and Clarke 1996, Kardomateas and Schmueser 1988, Gummadi and Hanagud 1995), their implementation can be very expensive for practical applications. The layer-wise approach (Barbero and Reddy 1991) is an alternative since it is capable of modeling displacement discontinuities. However, the computational effort increases with the number of plies. Recently, a refined higher order theory, developed by Chattopadhyay and Gu (1994), was shown to be both accurate and efficient for modeling delamination in composite plates and shells of moderately thick construction. This theory has also been shown to agree well with both elasticity solutions (Chattopadhyay and Gu 1996) and experimental results (Chattopadhyay and Gu 1998).

Preliminary research (Keilers and Chang 1995) has been conducted on the use of smart materials for detecting pre-existing delamination. However, the mathematical models used in these works are simply classical theory-based approaches, which exclude the transverse shear effects. The importance of transverse shear deformation in composite laminates has been identified by many researchers. As

† Professor, Associate Fellow AIAA, Member SPIE, ASME, AHS, ISSMO, AAM.
‡ Graduate Research Associate, Member AIAA.
§ Postdoctoral Fellow, Member AIAA, ASME.

0964-1726/99/010092+08$19.50 

much as 50% deviations in structural response have been reported in thick constructions (Barbero and Reddy 1991, Chattopadhyay and Gu 1994, Chattopadhyay and Seeley 1996, 1997). Therefore, the objective of the current research is modeling the dynamic response of delaminated smart composite cross-ply beams using a refined higher order theory.

A higher order theory-based finite element model is presented for delaminated smart composite cross-ply beams. The model properly takes into account the distributed nature of the presence of discrete delaminations, actuators and sensors. Since the relationships between the induced strain due to actuation and the applied electric field are nonlinear in nature (Crawley and Anderson 1989), a new formulation is presented to include these nonlinear induced strain effects. A control algorithm is implemented for vibration reduction.

## 2. Higher order theory based formulation

A general higher order displacement field is extended to model composite cross-ply beams with induced strain actuations due to piezoelectric materials (figure 1). The in-plane displacements are assumed to be effectively expressed by a cubic function through the thickness ($z$) and the transverse displacement is assumed to be independent of $z$. To model delamination in such structures, the general displacement field is defined as

$$U(x,z,t) = u(x,t) + (z-c)\left[\psi(x,t) - \frac{\partial w(x,t)}{\partial x}\right] + (z-c)^2\phi(x,t) + (z-c)^3\varphi(x,t) \qquad (1)$$
$$W(x,z,t) = w(x,t)$$

where $U$ and $W$ are the in-plane and out-of-plane displacements at a point $(x,\ z)$, $u$ and $w$ denote the midplane displacements, $\psi$ represents the rotation of the midplane, $\phi$ and $\varphi$ are the higher order terms. The quantity $c$ denotes the distance between the global midplane of undelaminated laminates and the local midplane of the sublaminate.

For an anisotropic elastic body, the constitutive relations among the stress, strain, charge and electric field can be derived from the electric enthalpy density function given as follows

$$H\left(\varepsilon_{ij},\ E_i\right) = \tfrac{1}{2}c_{ijkl}\varepsilon_{ij}\varepsilon_{kl} - e_{ijk}E_i\varepsilon_{jk} - \tfrac{1}{2}k_{ij}E_iE_j \qquad (2)$$

where $\varepsilon_{ij}$ and $E_i$ are components of the strain tensor and electric field vector, respectively and $c_{ijkl}$, $e_{ijk}$, and $k_{ij}$ are the elastic, piezoelectric and dielectric permittivity constants, respectively. The charge and stress are then determined as

$$D_i = -\frac{\partial H}{\partial E_i} \qquad (3)$$

$$\sigma_{ij} = \frac{\partial H}{\partial \varepsilon_{ij}}. \qquad (4)$$

For an orthotropic composite beam with piezoelectric layers, the constitutive relationships can be simplified as

$$\begin{bmatrix}\sigma_x\\ \tau_{xz}\end{bmatrix}_k = \begin{bmatrix}\bar{Q}_{11} & 0\\ 0 & \bar{Q}_{55}\end{bmatrix}\begin{bmatrix}\varepsilon_x - \Lambda_x\\ \gamma_{xz}\end{bmatrix} \qquad (5)$$

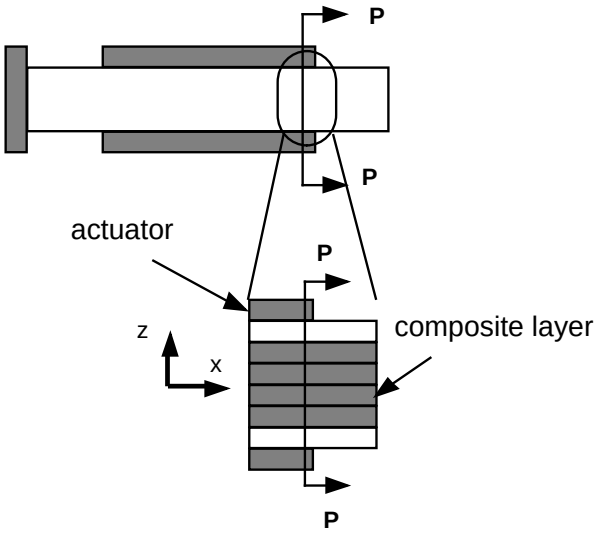


**Figure 1.** Cantilever composite laminate with piezoelectic actuators.

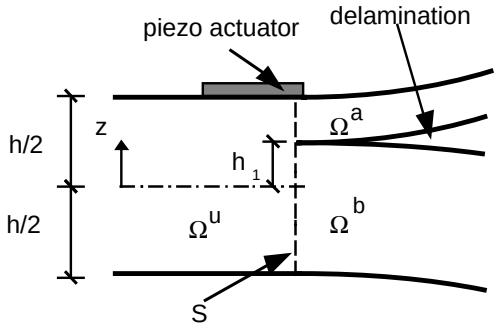


**Figure 2.** Laminate cross section.

$$D_{3_k} = \bar{Q}_{11}d(\varepsilon)\varepsilon_{x_k} \qquad (6)$$

where $\Lambda_x$ are the induced strains ($\Lambda_x = d(\varepsilon)E_3$).

To account for the delamination effects, it is necessary to partition the laminate into several different regions as shown in figure 2. These regions include the nondelaminated region $\Omega^u$, the region above the delamination $\Omega^a$ and the region below the delamination $\Omega^b$. The interface between the nondelaminated region and the delaminated region, indicated by the dashed line in figure 2, is denoted $S$. The general form of the higher order displacement field (equation (1)) is independently applied to each of these regions to describe displacements which account for slipping and separation due to the delamination. However, this displacement field must satisfy the traction-free boundary conditions at the top and bottom surfaces of the beam ($z = \pm h/2$) as well as on the delamination interface ($z = h_1$) in the delaminated region. That is,

$$\tau_{xz}(x, z*) = 0 \qquad x \in \Omega^r$$
$$\left(r = u, a, b, \qquad z^* = \pm h, h_1\right) \qquad (7)$$

in which the superscript $r$ corresponds to either the nondelaminated region ($u$), or the regions above and below the debonding ($a$ and $b$), respectively. For orthotropic plates, these conditions are equivalent to the requirement that

the corresponding transverse shear strains be zero on these surfaces. A refined displacement field is then obtained by applying these boundary conditions in each region as follows

$$U^r = u^r + (z - c^r)\left(\psi^r - \frac{\partial w^r}{\partial x}\right) - \frac{4(z-c^r)^3}{3(d^r)^2}\psi^r \quad (r = u, a, b)$$
$$W^r = w^r \tag{8}$$

where $c^r$ is the local midplane and $d^r$ is the local thickness of the region. With the identification of the higher order terms, the variables in the generalized displacement field are reduced. It is important to note that the total thickness of the beam, $h$, may vary due to the presence of surface bonded sensors/actuators.

Additional continuity conditions must be imposed to ensure the continuity of displacements at the interface of the nondelaminated and the delaminated regions ($S$) as shown in figure 2. The continuity conditions at the interface of the nondelaminated and the delaminated regions are imposed as follows

$$\begin{aligned} U^u &= U^a \\ W^u &= W^a \\ U^u &= U^b \\ W^u &= W^b \end{aligned} \qquad x \in S. \tag{9}$$

The above equations can be exactly satisfied with the classical theory since it assumes a linear displacement distribution through the thickness. However, the displacement distribution using the refined theory is nonlinear and therefore equations (9) can be approximated at the local midplane as follows

$$\begin{aligned} &U^u = U^a \qquad W^u = W^a \\ &\frac{\partial U^u}{\partial z} = \frac{\partial U^a}{\partial z} \qquad \frac{\partial^2 U^u}{\partial z^2} = \frac{\partial^2 U^a}{\partial z^2} \qquad z = c^a \\ &U^u = U^b \qquad W^u = W^b \qquad x \in S \\ &\frac{\partial U^u}{\partial z} = \frac{\partial U^b}{\partial z} \qquad \frac{\partial^2 U^b}{\partial z^2} = \frac{\partial^2 U^b}{\partial z^2} \qquad z = c^b \end{aligned} \tag{10}$$

Using equations (10), the relations between the displacement fields, defined in the different regions, at region interface $S$ can now be derived as follows

$$\begin{aligned} u^a &= u^u + \frac{1}{2}\left(\frac{h}{2} + h_1\right)\left(\psi^u - \frac{\partial w^u}{\partial x}\right) - \frac{\left(\frac{h}{2} + h_1\right)^3}{6h^2}\psi^u \\ w^a &= w^u \qquad \psi^a = \psi^u \qquad \frac{\partial w^a}{\partial x} = \frac{\partial w^u}{\partial x} \\ u^b &= u^u + \frac{1}{2}\left(\frac{h}{2} - h_1\right)\left(\psi^u - \frac{\partial w^u}{\partial x}\right) - \frac{\left(\frac{h}{2} - h_1\right)^3}{6h^2}\psi^u \\ w^b &= w^u \qquad \psi^b = \psi^u \qquad \frac{\partial w^b}{\partial x} = \frac{\partial w^u}{\partial x}. \end{aligned} \tag{11}$$

## 3. Nonlinear piezoelectric actuation

It is assumed that the piezoelectric actuators are surface bonded on the composite laminate. Therefore, the piezoelectric material can be treated as an additional surface layer. The electro-mechanical coupling between the applied electric field and the induced strain in the piezoelectric material is governed by the coupling coefficients, $d$, which represent piezoelectric material properties. According to Crawley and Lazarus (1991), the coefficient depends on the actual strain in the actuator as well. That is,

$$\Lambda = d(\varepsilon)E_3 \tag{12}$$

where $E_3$ is the applied electric field through the thickness of the actuator. However, due to the weak nonlinearity, equation (12) can be rewritten using first order terms in Taylor series expansion. That is,

$$\Lambda = \left(d_0 + d_1\varepsilon + \tfrac{1}{2}\varepsilon^2 + \ldots\right)E_3 = d_0 E_3 + d_1 \varepsilon E_3. \tag{13}$$

The coefficients $d_0$ and $d_1$ can be identified using functional relationships of the strain versus electric field obtained from experimental data of an unconstrained piezoelectric actuator.

## 4. Control algorithm

Since the piezoelectric sensors can accurately detect the strain rate when they are connected with a current amplifier and proportional feedback is the simplest to apply for structural vibration control, a piezoelectric sensor model is developed here for monitoring the proportional variables that are necessary for control feedback. When the $k$th piezoelectric sensor layer is deformed, it accumulates an electric charge on its surface electrode that is given by

$$q_k(t) = \int_A \int_z D_{3_k} \mathrm{d}z\mathrm{d}A = \int_A \int_z \bar{Q}_{11} d_{31} \varepsilon_{x_k} \mathrm{d}z\mathrm{d}A. \tag{14}$$

The current developed from the electric charge is obtained by differentiating the charge equation (equation (14)) with respect to time.

$$i_k(t) = \frac{\mathrm{d}q_k(t)}{\mathrm{d}t} = \int_A \int_z \bar{Q}_{11} d(\varepsilon) \frac{\mathrm{d}\varepsilon_{x_k}}{\mathrm{d}t} \mathrm{d}z\mathrm{d}A. \tag{15}$$

With a design of control law using the Lyapunov direct method, the beam stability in the Lyapunov sense is guaranteed if the feedback actuator voltage is selected as

$$E_{3k}(t) = G i_k(t) = G \int_A \int_z \bar{Q}_{11} d(\varepsilon) \frac{\mathrm{d}\varepsilon_{x_k}}{\mathrm{d}t} \mathrm{d}z\mathrm{d}A \tag{16}$$

with gain $G > 0$.

## 5. Finite element modeling

The finite element method (FEM) is used to implement the refined higher order theory since it allows for the analysis of practical geometries and boundary conditions. The continuity conditions presented in equations (11), between the nondelaminated region ($\Omega^u$) and delaminated regions ($\Omega^a$, $\Omega^b$), are applied to the finite element degrees of freedom at the interface of the nondelaminated and delaminated regions ($S$) by first presenting these discretized conditions in matrix form as follows.

$$\boldsymbol{u}_s^k = \mathbf{T}^k \boldsymbol{u}_s^u \qquad k = a, b \tag{17}$$

**Table 1.** Material properties.

| | $E_1$ (GPa) | $E_2$ (GPa) | $\upsilon_{12}$ | $G_{12}$, $G_{13}$ (GPa) |
|---|---|---|---|---|
| Graphite/epoxy | 134.4 | 10.3 | 0.33 | 5 |
| PZT | 63 | 63 | 0.33 | 24.2 |
| | $G_{23}$ (GPa) | $\rho$ ($\times 10^3$ kg m$^{-3}$) | $d_0$ ($\times 10^{-12}$ m V$^{-1}$) | $d_1$ ($\times 10^{-7}$ m V$^{-1}$) |
| Graphite/epoxy | 2 | 1.477 | | |
| PZT | 24.2 | 7.6 | 247 | 8.38 |

**Table 2.** First natural frequency for delamination along the midplane.

| Delamination length (mm) | Experiment 1 (Hz) | Experiment 2 (Hz) | Experiment 3 (Hz) | Existing model (Hz) | Current model (Hz) |
|---|---|---|---|---|---|
| 0 | 79.875 | 79.875 | 79.750 | 82.042 | 81.859 |
| 25.4 | 78.376 | 79.126 | 77.001 | 80.133 | 78.872 |

where

$$\boldsymbol{u}_s^k = \left[u^k,\ \psi^k,\ w^k,\ z\frac{\partial w^k}{\partial x}\right]_s^T$$
$$\boldsymbol{u}_s^u = \left[u^u,\ \psi^u,\ w^u,\ \frac{\partial w^u}{\partial x}\right]_s^T \qquad (18)$$
$$\mathbf{T}_k = \begin{bmatrix} 1 & h_k - \frac{4h_k^3}{3h^2} & 0 & -h_k \\ 0 & 1 & 0 & 0 \\ 0 & 0 & 1 & 0 \\ 0 & 0 & 0 & 1 \end{bmatrix}$$
$$h_k = \tfrac{1}{2}\left(\tfrac{h}{2} + h_1\right) \quad \text{when } k = a$$
$$h_k = \tfrac{1}{2}\left(\tfrac{h}{2} - h_1\right) \quad \text{when } k = b.$$

Using equations (18), the node variables defined in the delaminated region can easily be expressed in terms of those defined in the nondelaminated region at the region interface.

The finite element equations are derived using the discretized form of Hamilton principle, which is stated as follows.

$$\delta\Pi = \int_{t_1}^{t_2} \sum_{e=1}^{N_e} \left[\delta K^e - \delta U^e + \delta W^e\right] \mathrm{d}t = 0 \qquad (19)$$

where $t_1$ and $t_2$ are the initial and the final times, respectively and $\delta K^e$, $\delta U^e$ and $\delta W^e$ represent the elemental variations in the kinetic, the strain and the potential energies, respectively. The finite element equations are formulated as follows.

$$\int_{t_1}^{t_2} \sum_{e=1}^{N_e} \left[\delta \boldsymbol{u}^e \mathbf{M}^e \ddot{\boldsymbol{u}}^e + \delta \boldsymbol{u}^e \mathbf{K}^e \boldsymbol{u}^e - \delta \boldsymbol{u}^e \left(\boldsymbol{F}^e + \boldsymbol{F}_p^e\right)\right] = 0 \qquad (20)$$

where $N_e$ is the number of elements, an overdot indicates a derivative with respect to time and $\boldsymbol{u}^e$ represents the nodal generalized displacement vector for each element. The mass matrix, $\mathbf{M}^e$, is formulated using the material density and the element shape functions. The stiffness matrix, $\mathbf{K}^e$, includes the stiffness of the smart beam and the additional stiffness modification due to nonlinear actuation. Two force vectors are formulated for the distributed load, $\boldsymbol{F}^e$, and the piezoelectric forces $\boldsymbol{F}_p^e$. The global finite element equations of motion are then expressed as follows.

$$\mathbf{M}\ddot{\boldsymbol{u}} + \mathbf{K}\boldsymbol{u} = \boldsymbol{F} + \boldsymbol{F}_p \qquad (21)$$

where the quantities $\mathbf{M}$, $\mathbf{K}$, $\boldsymbol{F}$ and $\boldsymbol{u}$ denote the mass and the stiffness matrices, the force vector due to a distributed load and the nodal displacement vector, respectively. The quantity $\boldsymbol{F}_p$ is the force vector due to piezoelectric actuation. Linear shape functions are used for the in-plane displacements and rotations ($u$, $\psi$) while a four term cubic polynomial is used for the transverse displacements ($w$). The resulting two noded beam elements are computationally efficient and contain four degrees of freedom at each node.

## 6. Numerical results

Numerical results are presented first to compare the higher order theory with published experimental and analytical results to ascertain its validity. Next, dynamic response and vibration control using piezoelectric actuation are presented for a cantilever composite beam with varying delamination length. Differences between the developed higher order theory and the first order theory are also discussed. $[0^\circ/90^\circ/0^\circ/90^\circ]_s$ graphite/epoxy laminates with surface bonded piezoelectric actuator pairs are used in the analysis. The material properties used for the smart composite beam are listed in table 1, where $E$ is the Young's modulus and $\upsilon$ is the Poisson ratio. Cross-ply beams with length $L = 0.127$ m, thickness $h = 0.001\,016$ m and width $b = 0.0127$ m are considered. The piezoelectric actuator pairs have dimensions of $L_p = 0.0127$ m, $h_p = 0.000\,254$ m and $b_p = 0.0127$ m, located in different positions (figure 1).

The results from the current approach are compared to finite element results and experimental data obtained by Shen and Grady (1991) as shown in table 1. The finite element model in that research is based on the Timoshenko beam theory. Delamination lies on the midplane of the beam and is located at midspan. As shown in table 2, the natural frequencies obtained from the higher order theory-based finite element approach show much better correlations with experimental data, compared to the existing finite element results, especially in the delaminated case. This indicates that the higher order theory-based model provides improved accuracy while maintaining the same computational efficiency since the number of degrees of freedom per node is the same as in the Timoshenko beam theory-based finite element.

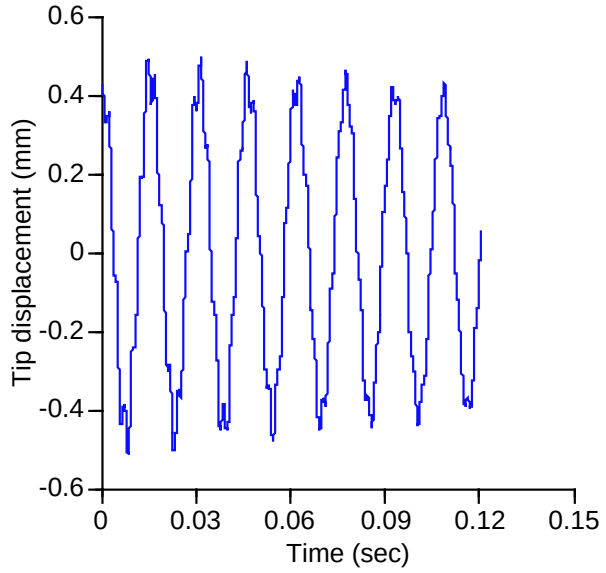


**Figure 3.** Time history of tip displacement, no control, no delamination.

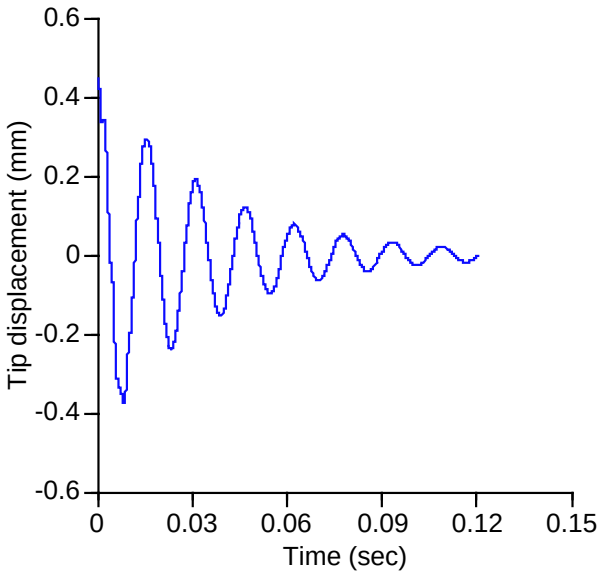


**Figure 4.** Time history of tip displacement, with control, no delamination.

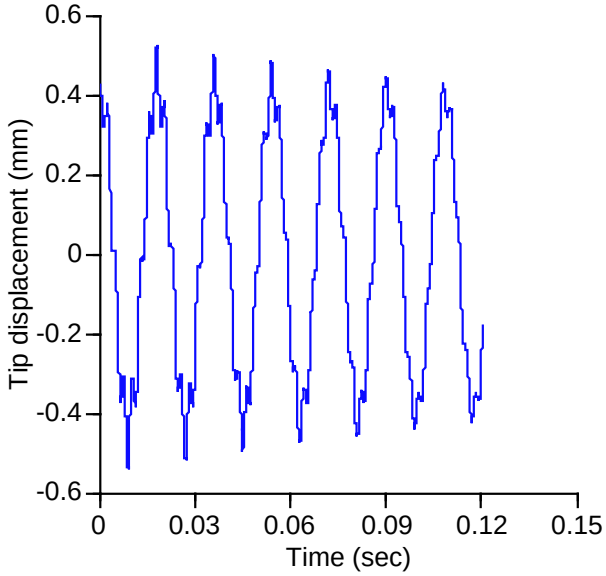


**Figure 5.** Time history of tip displacement, no control, with delaminations.

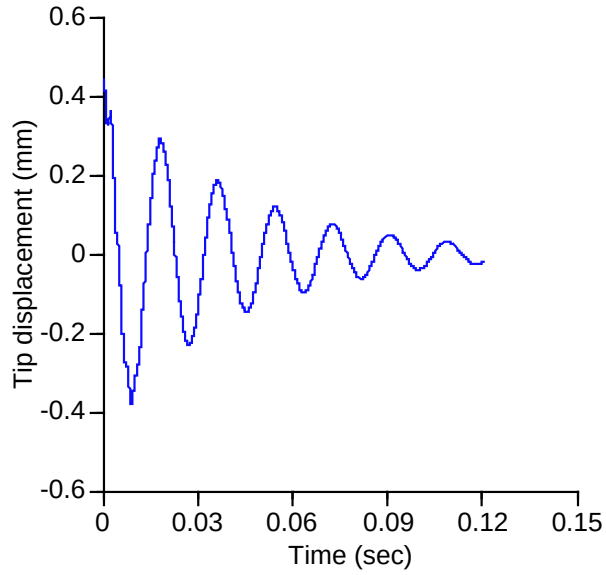


**Figure 6.** Time history of tip displacement, with control, with delaminations.

The effect of closed loop control due to piezoelectric actuation is investigated. The beam is released from an initially bent position, which is produced by a piezoelectric actuation due to 127 V. Ten equal-sized elements are used which are numbered from the clamped end to the free end. The actuator pairs are located at the top and the bottom surfaces of the second, third, fifth, sixth, eighth and ninth elements (figure 1). The internal structural damping is assumed to be 0.3% of critical damping for each normal coordinate. Figures 3 and 4 present the dynamic responses of nondelaminated smart composite beams without and with closed loop control, respectively. It is seen that the actuators effectively damp out the beam vibrations with the use of the closed loop control. The dynamic responses of delaminated smart composite beams are also presented in figures 5 and 6 for cases without and with feedback control, respectively. The same beam configurations and initial conditions are used as in the previous example. Multiple delaminations are assumed which are located in the first four elements. Each of these delaminations is assumed to lie on the midplane of the beam, and the delamination length is assumed equal to half the element length. With delaminations, the amplitude of vibrations becomes larger as shown in figure 5, compared to the nondelaminated case presented in figure 3. Moreover, the presence of delaminations also weakens the control authorities. As shown in figures 6 and 4 the beam vibrations are being damped out at a slower rate in the presence of delamination (figure 6).

Finally, the first two modes of vibration are presented

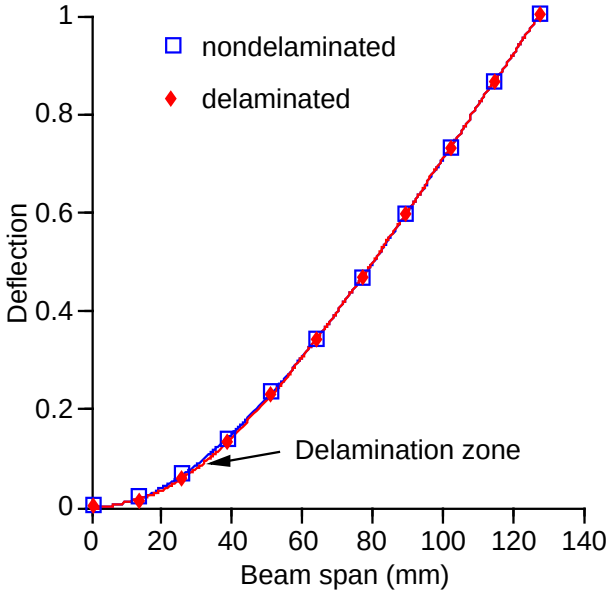


**Figure 7.** First mode of vibration (with and without delamination).

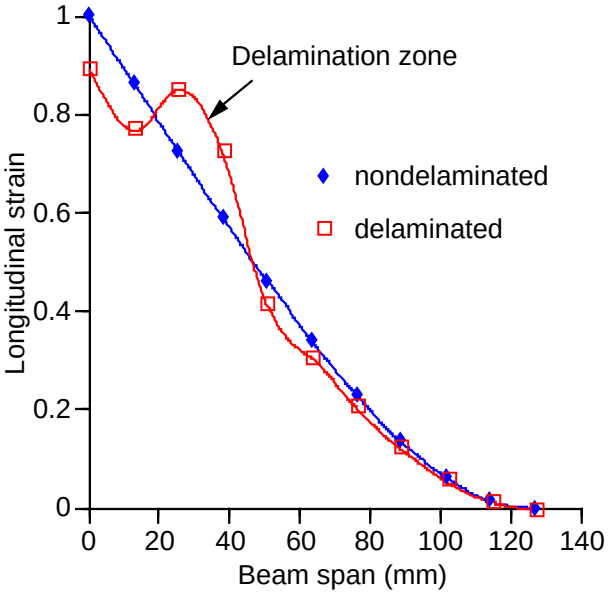


**Figure 9.** Longitudinal strain corresponding to first mode of vibration.

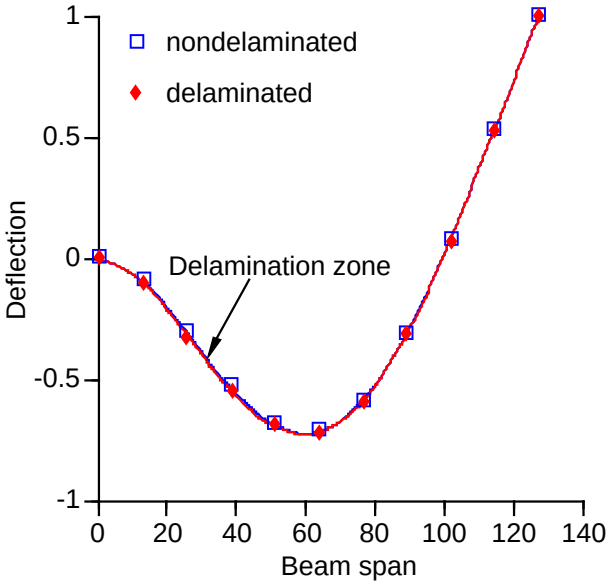


**Figure 8.** Second mode of vibration (with and without delamination).

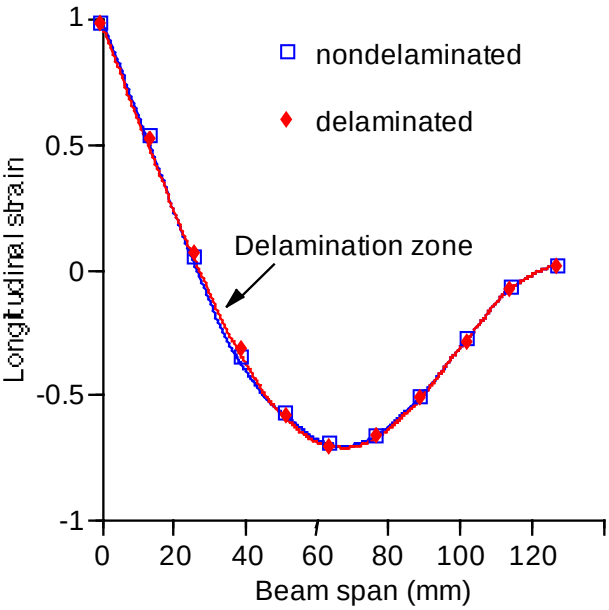


**Figure 10.** Longitudinal strain corresponding to second mode of vibration.

in figures 7 and 8, while the corresponding longitudinal strains are shown in figures 9 and 10 for both nondelaminated and delaminated cases. In this study a single delamination of length 0.006 35 m is placed in the midplane starting at 0.031 75 m from the clamped end. For a small delamination, it is observed that the classical mode shapes remain almost unchanged. However, the longitudinal strains corresponding to these modes indicate that the strain is a more sensitive measure of delamination and can be used as a more effective parameter in detecting delaminations in composites. For large delaminations, however, the mode shapes are largely influenced by an overall loss of rigidity in the beam (figures 11 and 12). In this last case the delamination length is assumed to be 0.0508 m and is located at midspan.

## 7. Concluding remarks

A general framework has been developed for the analysis of smart composite beams with surface-bonded piezoelectric actuators and sensors in the presence of delamination. A

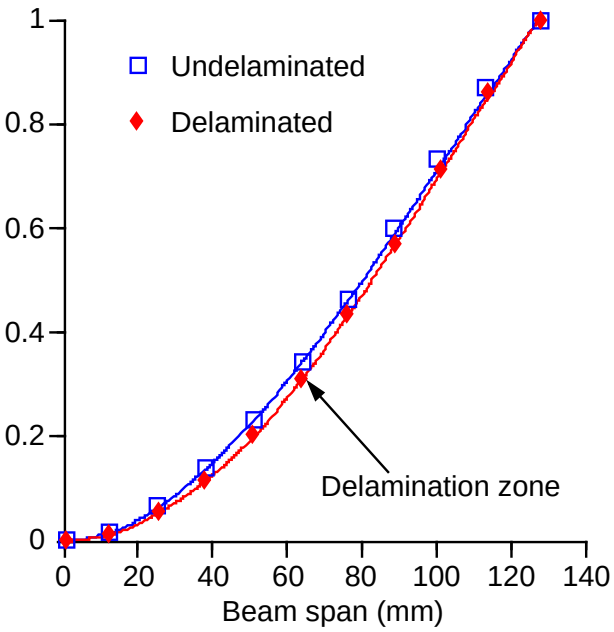


**Figure 11.** First mode of vibration—multiple delaminations.

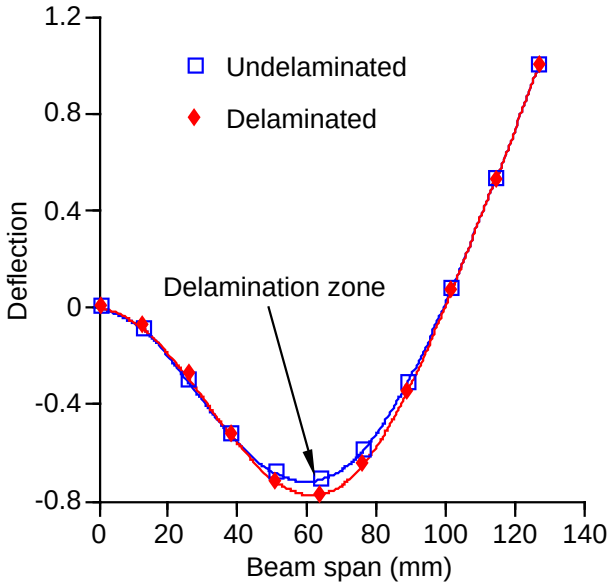


**Figure 12.** Second mode of vibration—multiple delaminations.

refined higher order theory has been used that accurately captures the transverse shear deformation through the thickness of the smart composite laminate while satisfying the stress-free boundary conditions on the free surfaces, including the delaminated region. The presence of pre-existing delaminations in the composite laminate at the layer interface was studied. The following important observations were made from this study:

(a) The developed theory correlates well with experimental results.

(b) Delaminations weaken the beam structures, produce larger vibration amplitude, and reduce the closed loop control authority.

(c) Insignificant changes are observed in classical mode shapes when delamination size is very small.

(d) Significant changes are observed in the longitudinal strain distribution due to delamination. This indicates that strain can be a more effective measure in the detection of delamination in a composite beam.

## Acknowledgments

The research was supported by the Air Force Office of Scientific Research, grant number: F49620-96-0195, technical monitor Dr Brian Sanders. The authors would like to thank Dr Charles E Seeley, for helpful discussions.

## References

Barbero E J and Reddy J N 1991 Modeling of delamination in composite laminates using a layer-wise plate theory *Int. J. Solids Struct.* **28** 373–88

Chandrashekhara K and Agarwal A N 1993 Active vibration control of laminated composite plates using piezoelectric devices: a finite element approach *J. Intell. Mater. Syst. Struct.* **4** 496–508

Chattopadhyay A and Gu H 1994 A new higher-order plate theory in modeling delamination buckling of composite laminates *AIAA J.* **32** 1709–18

——1996 An experimental investigation of delamination buckling and postbuckling of composite laminates *Proc. 14th Army Symp. on Solid Mechanics (Myrtle Beach, SC, 1996)* pp 306–13

——1998 Elasticity solution for delamination buckling of composite plates *AIAA J.* **36** 1529–34

Chattopadhyay A and Seeley C E 1996 A higher order theory for modeling composite laminates with induced strain actuators *Composites* B **28** 243–52

——1997 Experimental investigation of composites with piezoelectric actuation and debonding *Proc. Int. Mechanical Engineering Congr. Exposition Winter Annu. Meeting ASME: Adaptive Structures and Material Systems Symp. (Dallas, TX, 1997)* pp 316–25

Crawley E F and Anderson E H 1989 Detailed models of piezoelectric actuation of beams *Proc. 30th AIAA/ASME/ASCE/AHS/ASC Structures, Structural Dynamics and Materials Conf. (Mobile, AL, 1989)* pp 2000–10

Crawley E F and Lazarus K B 1991 Induced strain actuation of isotropic and anisotropic plates *AIAA J.* **29** 944–51

Gummadi L N B and Hanagud S 1995 Vibration characteristics of beams with multiple delaminations *Proc. 36th AIAA/ASME/ASCE/AHS/ASC Structures, Structural Dynamics and Materials Conf.—Adaptive Structures Forum (New Orleans, LA, 1995)* pp 140–50

Kardomateas G A and Schmueser M 1988 Buckling and postbuckling of delaminated composites under compressive loads including transverse shear effects *AIAA J.* **26** 337–43

Keilers C H and Chang F K 1995 Identifying delamination in composite beams using built-in piezoelectric: part I—experiments and analysis; part II—an identification method *J. Intell. Mater. Syst. Struct.* **5** 649–63

Lee C K 1990 Theory of laminated piezoelectric plates for the design of distributed sensors/actuators. Part 1: governing equations and reciprocal relationships *J. Acoust. Soc. Am.* **87** 1144–58

Lee H J and Saravanos D A 1995 Coupled layerwise analysis of thermopiezoelectric smart composite beams *AIAA J.* submitted

Mitchell J A and Reddy J N 1995 A refined hybrid plate theory for composite laminates with piezoelectric laminae *Int. J. Solids Struct.* **32** 2345–67

Pavier M J and Clarke M P 1996 A specialized composite plate element for problems of delamination buckling and growth *Composite Struct.* **35** 45–53

Reddy J N 1990 A general non-linear third-order theory of plates with moderate thickness *Int. J. Non-Linear Mech.* **25** 677–86

Robbins D H and Reddy J N 1991 Analysis of piezoelectrically actuated beams using a layerwise displacement theory *Comput. Struct.* **41** 265–79

Seeley C E and Chattopadhyay A 1996 Modeling delaminations in smart composite laminates *Proc. 37th AIAA/ASME/ASCE/AHS/ASC Structures, Structural Dynamics and Materials Conf.—Adaptive Structures Forum (Salt Lake City, UT, 1996)* pp 109–19

Seeley C E and Chattopadhyay A 1997 Modeling of smart composite laminates including debonding: a finite element approach *Proc. 38th AIAA/ASME/ASCE/AHS/ASC Structures, Structural Dynamics and Materials Conf.—Adaptive Structures Forum (Kissimmee, FL, 1997)*

Shen M H and Grady J E 1991 Free vibration of delaminated beams *Proc. 31st AIAA/ASME/ASCE/AHS/ASC Structures, Structural Dynamics and Materials Conf. (Baltimore, MD, 1991)*

Tzou H S and Zhong J P 1993 Electromechanics and vibrations of piezoelectric shell distributed systems *J. Dyn. Syst. Meas. Control* **115** 506–17

Whitcomb J D 1989 Three dimensional analysis of a postbuckled embedded delamination *J. Composite Mater.* **23** 862–89

Yang H T Y and He C C 1994 Three-dimensional finite element analysis of free edge stresses and delamination of composite laminates *J. Composite Mater.* **28** 1394–412